SSRG International Journal of Electrical and Electronics Engineering
ISSN: 2348-8379/ https://doi.org/10.14445/23488379/IJEEE-V12I6P113

Volume 12 Issue 6, 158-168, June 2025

Original Article

Flexible Bidirectional Converter Connecting DC and AC Microgrids for Smart Grid

Nguyen The Vinh

Automation and Robotics Laboratory, Faculty of Electronic Engineering I, Posts and Telecommunications Institute of Technology Hanoi, Vietnam.

Corresponding Author : vinhnt@ptit.edu.vn

Received: 09 April 2025 Revised: 11 May 2025 Accepted: 10 June 2025 Published: 30 June 2025

Abstract *- Currently, implementing a hybrid micro-power system in the power system has received significant attention from recent researchers. The flexible connection and exchange of energy in independent or grid-connected multi-microgrid systems is studied for multi-function converters. In addition, the issue of appropriate energy management, saving and stabilizing the power system from distributed energy sources (renewable energy sources) is necessary to provide continuous supply to the loads. The current power system has mixed DC and AC microgrids integrating many sub-grids. The energy exchange between those grids requires basic energy converters such as DC/DC, DC/AC and AC/DC. This work presents a multifunction converter structure that integrates a two-way power conversion method in grid-connected or independent DC/DC/AC/DC for microgrids. In this converter system, the non-isolated form uses two-way power electronic locking technology derived from the basic principle of Flyback, Boost, Buck and full bridge converters. The power grids consist of two DC microgrids and one AC microgrid capable of grid connection and independent operation. Flexible operation is realized with the combination of 3 microgrids, so the converter ensures each specific case for efficient energy use from distributed sources. The results of the simulation and experiment in the laboratory are compared.*

Keywords *- Bidirectional DC/DC converters, DC/AC converters, AC/DC converters, Batteries, Hybrid power systems*

1. Introduction

The current power system continuously changes in source and load according to the high-speed development and geographical area of the loads, as well as the concepts of microgrid and sub-grid [1-3]. The well-researched microgrid for low-voltage distribution systems that are directly connected to non-conventional distributed energy sources (PV, wind, fuel cells, micro-turbines, etc.), energy storage component [4]. The above grids can operate independently (referred to as stand-alone mode of operation) or synchronized with the grid (referred to as grid connection mode) [3]. The emergence of micro-power sources with grid-connected or off-grid load and energy storage integrated by power electronic converters that can control current and electricity Suitable voltage ensures power quality [5-7].

Furthermore, with a converter integrated with research-developed functions such as, the system for the converter will have many passive and power-consuming elements, modeling and control components more control. Solutions for different energy management and control strategies have been presented in the literature for the past decades [8-10], and progressive research is taking place in developed and developing countries that have developed to control mixed energy sources. Moreover, it ensures energy security for each country and the world. The different possible architectures of hybrid microgrids and converter topologies and configurations of the interconnecting converters are considered. In practice, many applications for voltage clamping systems use bidirectional DC/DC converters [11, 12], such as telecommunications, system computational power, electric vehicles and renewable energy systems.

Many researchers have studied the internal structures of two-way converters that can be grid-connected and independent for specific load applications. By the solutions of the power circuit structure, the control method for the energy conversion process all have disadvantages, such as poor energy conversion efficiency from source to load, high breakdown voltage conditions on the main switches and auxiliary switches, and high current ripple and voltage at the output. Currently, there are power circuit structures for high power values , such as clamped active bridge (DAB) converters presented in the document [13], but there are also complete bridge solutions such as the document [14], half-bridge types such as the document [15], push-pull solutions [16] or converters using resonant circuits such as the document [17, 18]. Bidretion DC/DC converters are very

common in industrial applications to manage power generation from renewable energy. The battery energy storage system (BESS) is charged and discharged from the operating principle of a DC/DC microgrid-connected or AC microgrid-connected DC/AC converter. This will be more advantageous than combining two DC converters mechanically to convert energy in each direction. Another issue is that performing the energy conversion process by electrical isolation by a medium-frequency transformer increases safety during operation and energy conversion.

Multi-port converters such as bidirectional DC/DC three-port converters connect power, DC lines and storage systems. The non-isolated converter allows the power to be transformed due to the transformation operation and the morphological operations of the system within the operating range of the transformation. Similarly, the bidirectional DC/DC multi-port converter, as shown, implements the principle of power allowable isolation. The problems of the above converters present a problem in solving the connection between the two DC and AC microgrids, such as [19, 20].

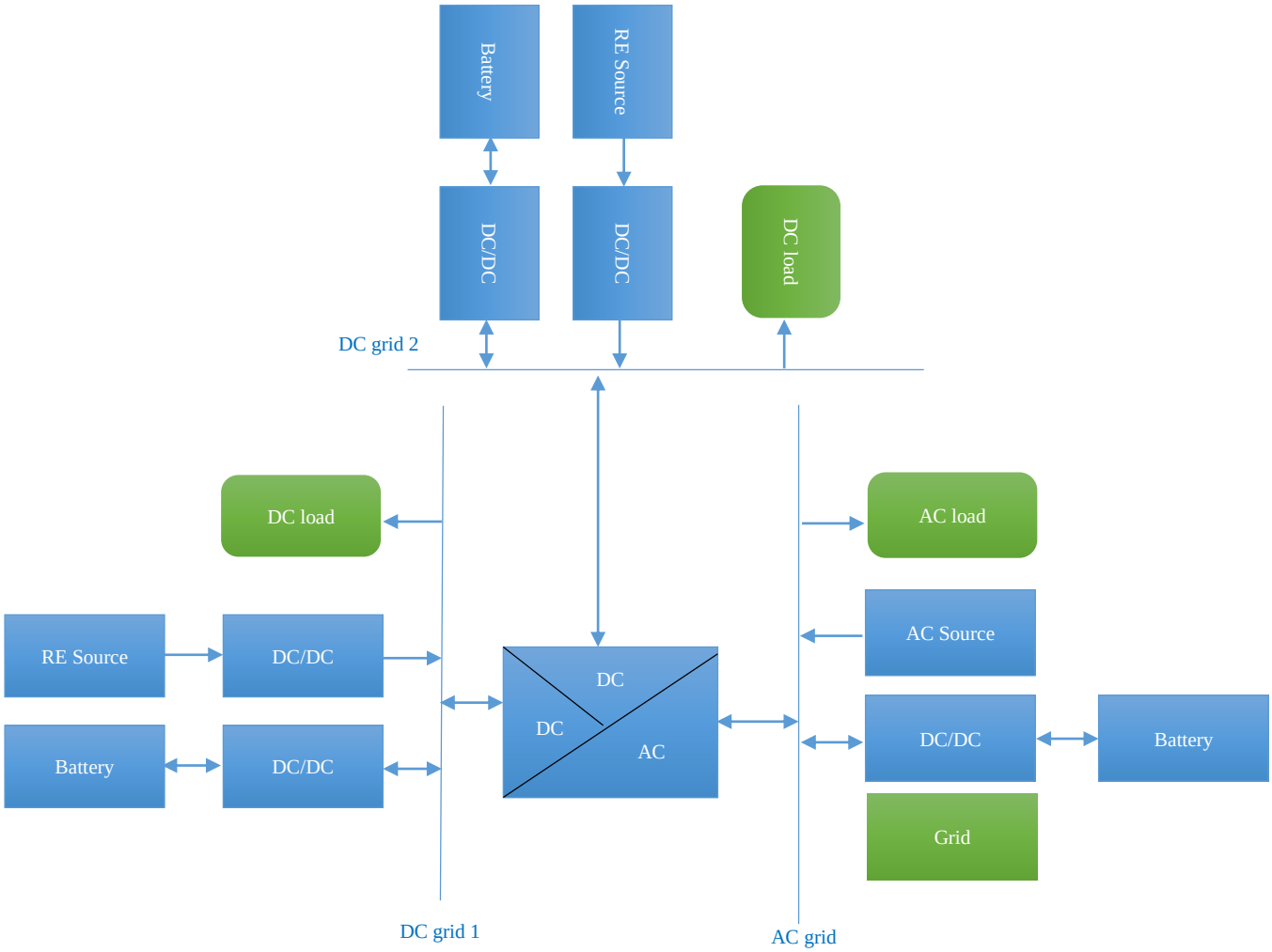

Fig. 1 Converter connection system block diagram

A hybrid Microgrid Three-Link converter (MGTL) system is proposed in this paper, as shown in Figure 1, in which the system consists of two DC and AC microgrids, renewable or distributed energy sources, storage systems, etc. are linked together by a DC/AC converter with bidirectional energy exchange. Each DC or AC microgrid comprises different basic components such as renewable energy sources (wind power, solar power, backup power generation system), DC load, AC load, and storage system. In addition, the AC microgrid has a grid connection described in Figure 1. This system can connect to the grid or operate independently. This system is connected to 3 microgrids by a bidirectional converter proposed in the article and presented and analyzed specifically in the following sections.

2. The Flexible Link Power MGLT Converter

The proposed converter connects to three DC and AC microgrids, as shown in Figure 2. This circuit diagram uses three bidirectional switches, S2, S3, S4 and five conventional switches, S1, S5-S8. There are two DC microgrids and one

AC microgrid. Step-up or step-down converters connect the DC grid to the AC grid. The connection between the two DC grids is by a DC chopper through a simple bidirectional switch S3. The proposed converter circuit shows a simple structure that minimizes the number of switches.

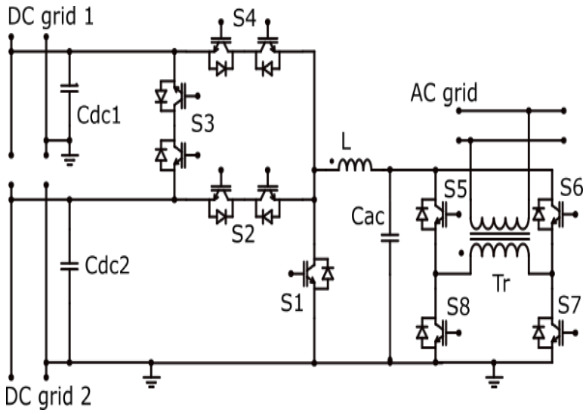

Fig. 2 Schematic diagram of the proposed converter MGTL

The buck DC/DC converter transfers power from DC grid 2 to the AC grid through an H-bridge converter (working as a DC/AC converter) isolated by the transformer. Tr DC grid 1 operates independently in this scenario. The current and voltage curves are modeled, as shown in Figure 4.

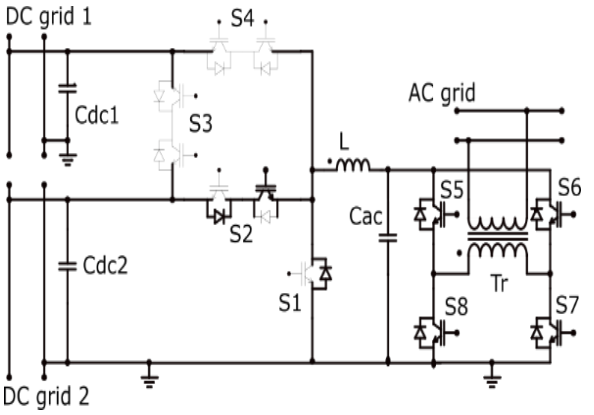

(a) scenario 1

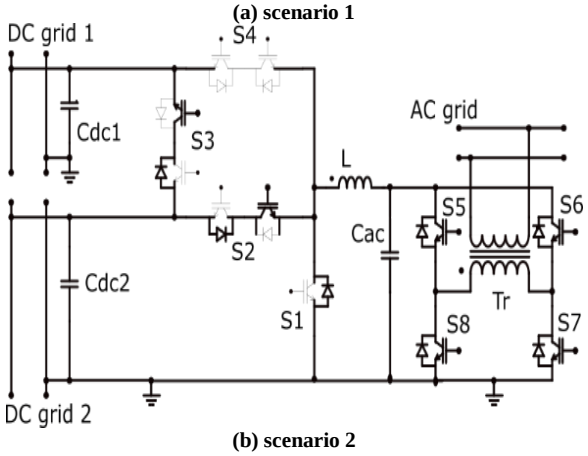

(b) scenario 2

Fig. 3 Operation diagram of scenarios 1 and 2 of the converter

The operation diagram of the converter in scenario 1 shows that there are 5 basic modes, such as buck DC/DC converter and H-bridge DC/AC converter, when the energy condition from the DC2 microgrid ensures the energy needed to supply to the load in the DC2 grid or the case where the load in the AC grid is given priority to provide continuous electrical energy.

The converters are connected between the DC2 and AC grids according to the inverter operation principle. The power transmitted from the DC2 grid to the AC grid is shown in Figure 3 (a). The voltage from S2 and the AC grid is shown in Figure 3 (b).

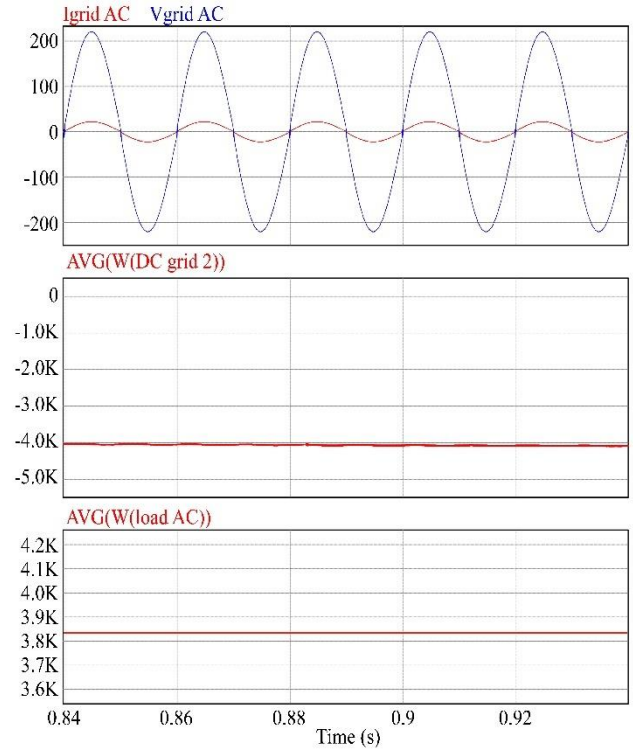

Fig. 4 Scenario 1 flow and pressure graph

The second scenario works when the energy is divided from the DC2 grid to the DC1 and AC grids when the S3 power switch is added, as shown in Figure 4. This scenario has the following assumptions from the grids: (1) when the source energy from the DC1 grid decreases due to weather effects, the stored energy is not enough to supply the load of the DC1 grid; (2) the load increases on the AC grid and the source remains unchanged; (3) the load on the DC2 grid decreases and the source energy increases, the stored energy is redundant.

The current and voltage graphs are shown in Figure 5. Showing the energy drop transmitted to the AC grid, the current and voltage on S2 and S3 are simulated to show values consistent with the working principles of the DC/DC and DC/AC converters.

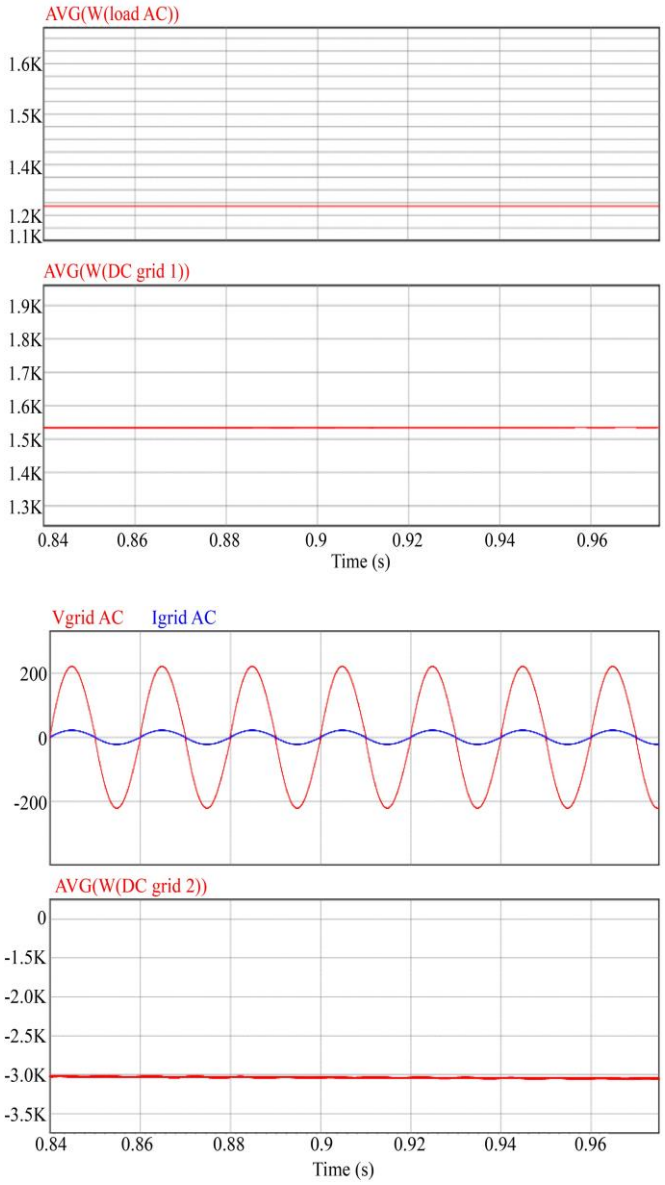

Fig. 5 Activity graph of scenario 2

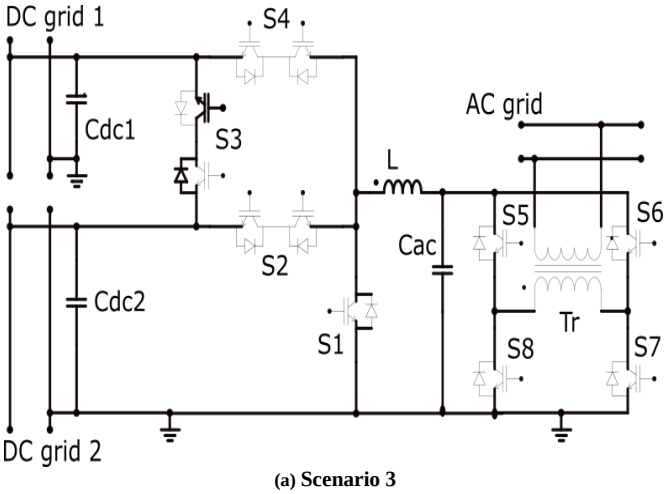

(a) Scenario 3

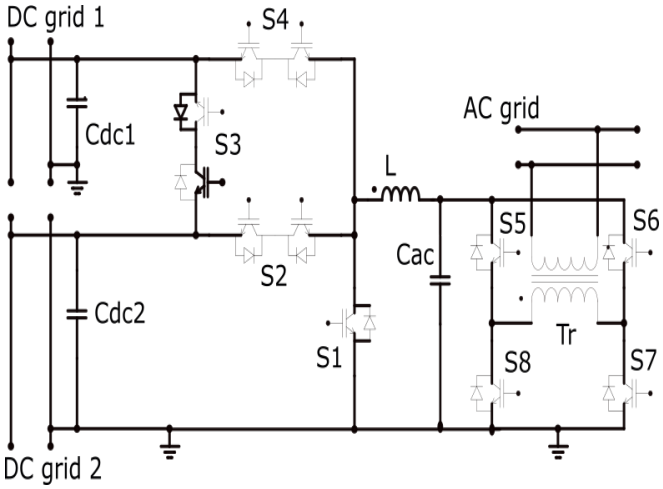

(b) Scenario 4

Fig. 6 Scenario 3 and 4 circuit principle

Figure 6 (a) and Figure 6 (b) illustrate the operation of the third scenario in the converter. In this scenario, energy is transferred from the DC2 grid to the DC1 grid. The AC grid operates independently, corresponding to the power electronic switches S2, S4, S5-S8 not operating. The DC1 microgrid needs to compensate for additional energy due to the decrease in power and the increase in load, and the stored energy source is not enough to meet the energy demand of the DC1 grid. In addition, the DC2 grid has excess energy from the power source and the stored source. The converter operates on the DC/DC conversion principle through voltage reduction through the switch S3 and the filter Ccd1.

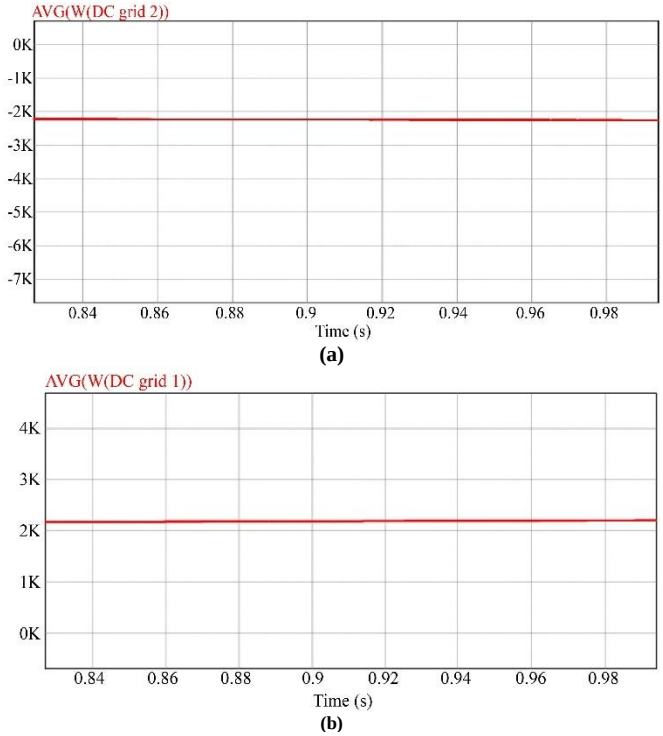

Fig. 7 Scenario 3 graph

The basic scenario 3 graph is like a DC/DC hashing circuit with a change in the average output voltage, as shown in Figure 7. There are 2 basic modes of closing and opening switch S3. The voltage on the DC1 grid will be smaller than the voltage on the DC2 grid. This is also a practical problem when the load on the DC1 grid suddenly increases, or the power suddenly decreases in a short period due to changes in the climate environment.

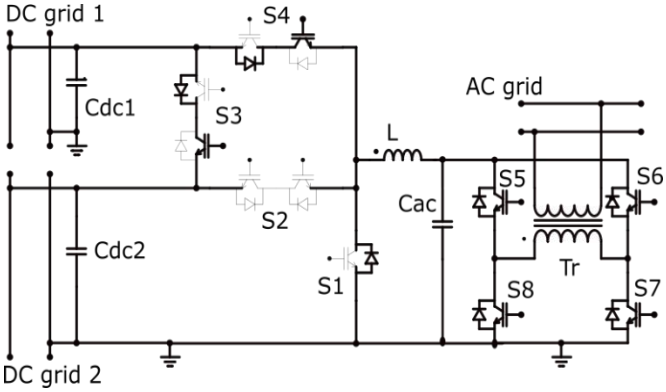

(a) Scenario 5

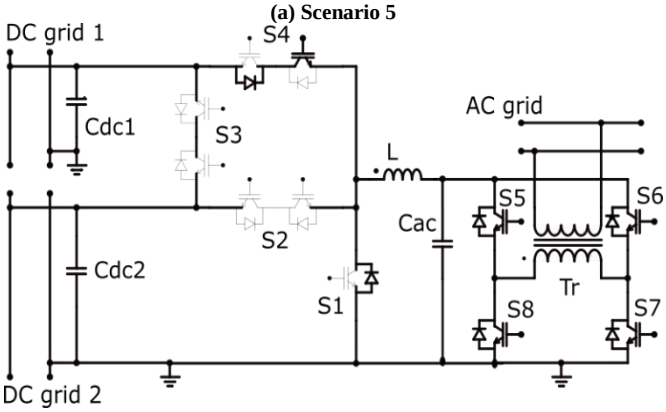

(b) Scenario 6

Fig. 8 Scenario 5 and 6 circuit principle

The fourth scenario is described in the principle of operation, as shown in Figure 8. The system supplies power from DC grid 1 to DC grid 2. The converter operates as in scenario 3 described above. The two-way power electronic switch S3 operates in reverse to scenario 3. Scenario 5 operates according to the principle shown in Figure 8 (a). The DC2 grid and AC grid are supplemented with additional energy from the DC1 grid when the load of DC2 and AC grids increases or the power of DC2 and AC grids decreases. The converter operates in 5 modes, as described in the current and voltage graphs in Figure 6. Corresponding to the Buck converter and H bridge operation combined with the S3 hashed rectifier. The working principle is the same as scenario 2 in the converter operation. Scenario 6 is like scenario 1 except that the power is supplied from the DC1 grid to the AC grid, as shown in Figure 8 (b). Figure 9 (a) describes the working principle of scenario 7. In this scenario, energy is converted from the AC grid to two grids, DC1 and DC2. The converter works as a rectifier (H-bridge converter), increasing the voltage using the Boost principle. The power electronic switches work as described in Figure 9 (a). The converter works in two basic stages described in Figure 9 (b); energy is converted from the AC grid to grid DC1. The first stage is the H-bridge rectifier of voltage and current, as described in Figure 10. The second stage is the DC/DC voltage increase with two basic modes, such as the Boost switch described in Figure 10 (b). The voltage on the switch S1 operating in this scenario is selected as the peak voltage value of the switch.

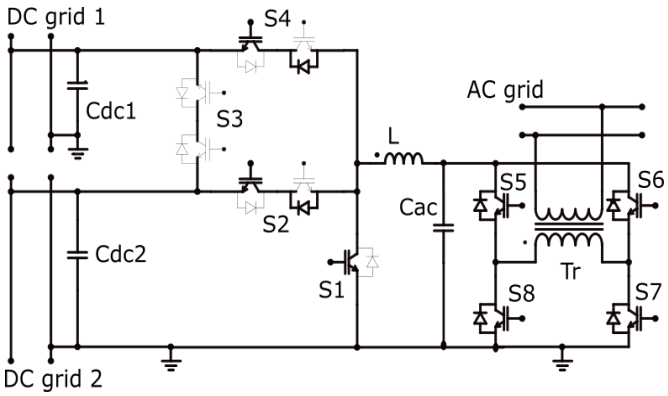

(a) Scenario 7

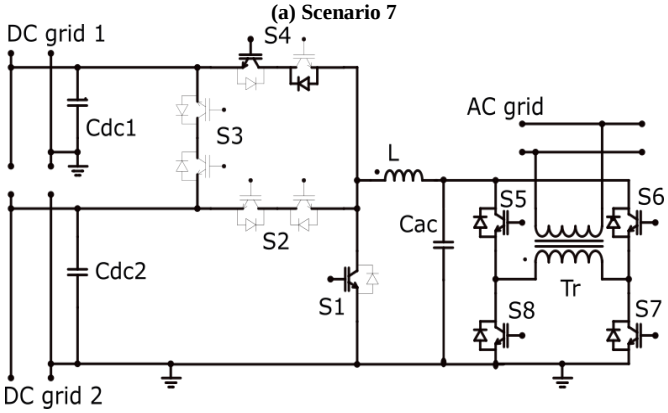

(b) Scenario 8

Fig. 9 Scenario 7 circuit principle

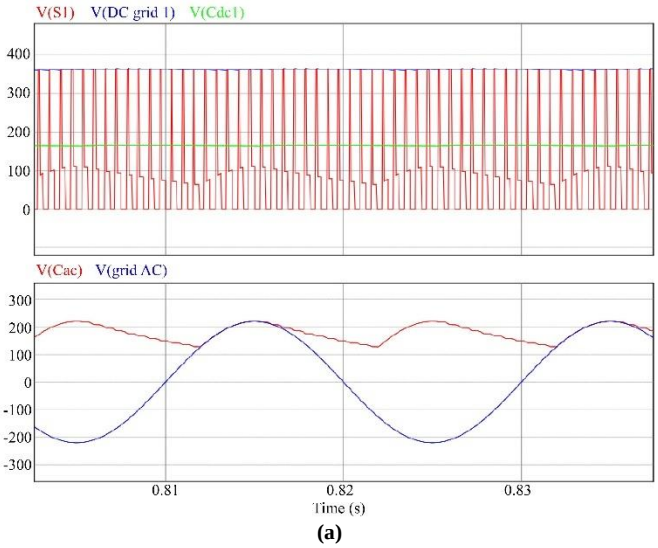

(a)

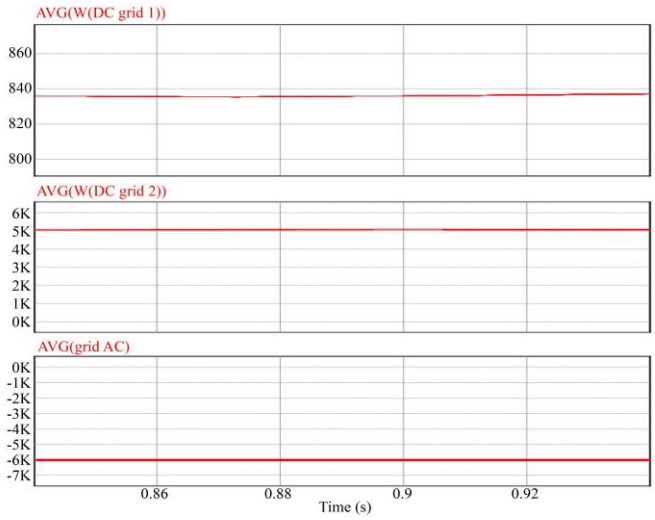

(b)

Fig. 10 Activity graph for scenario 7

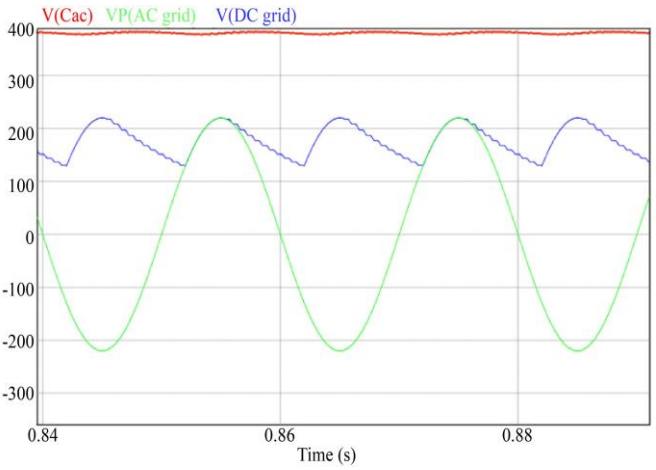

Fig. 11 Scenario 8 and Scenario 9 graphs as Scenario 8

Scenario 8, as shown in Figure 9 (b). The DC1 grid energy is supplemented from the AC grid because (1) the DC2 grid provides full power for the load and accumulates energy, (2) the DC1 grid is given priority for power (system operation), (3) the AC grid power is only supplied to a part of the system. The basic operation is the same as scenario 7. The only difference is that the S2 switch is inactive, and it is the case of selecting the current value for S1 or the same as scenario 9 shown in Figure 12 (a).

Figure 11 shows the current-voltage on elements S1 and S4, the power transmission from the AC grid to the DC grid1. The voltage is operated with the principle of increasing to the DC grid1 in scenario 8. Scenario 9 is replaced by switching S4 with S2.

There are cases in which the system has many microgrids that can operate independently of each other and exchange energy with each other, which can happen when the energy of a grid needs to supplement a large amount of energy infrequently, then the circuit principle as shown in Figure 17 is used. In the converter, the energy of the DC2 grid is supplemented by two DC1 grids and the AC grid. In this scenario 10 and 11, switches S2 and S4 are inactive.

The converter operates in two stages, as in scenario 7 and has additional energy from the DC1 grid through a DC/DC voltage regulator. Figure 13 (a) shows the current and voltage graph, and the power condition is in the equation in Table 1.

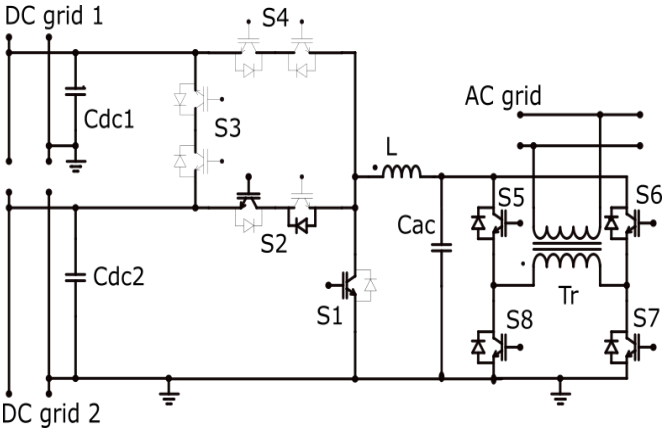

(a) Scenario 9

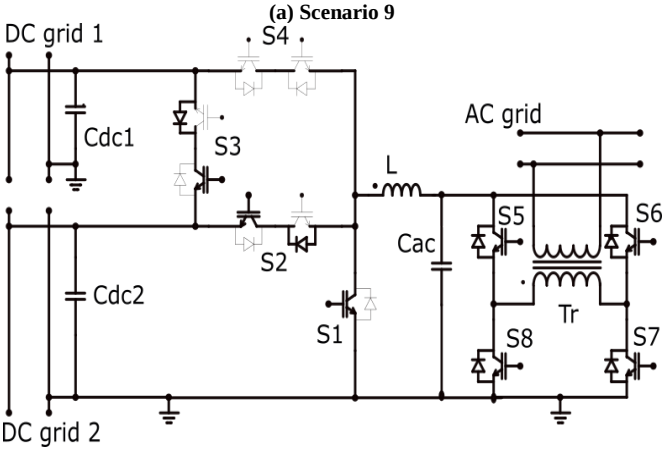

(b) Scenario 10

Fig. 12 Scenario 9 and 10 circuit principle

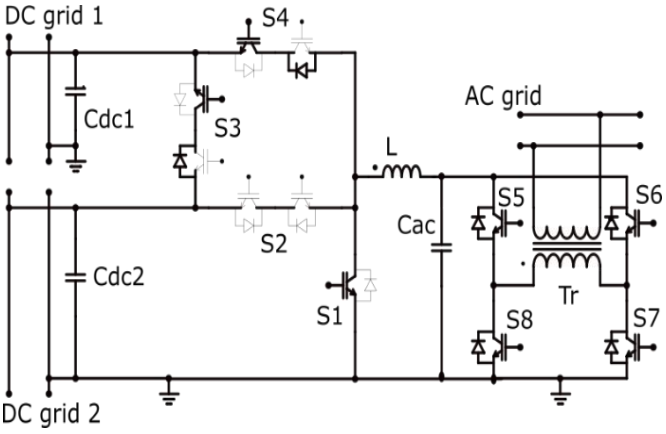

(a) Scenario 11

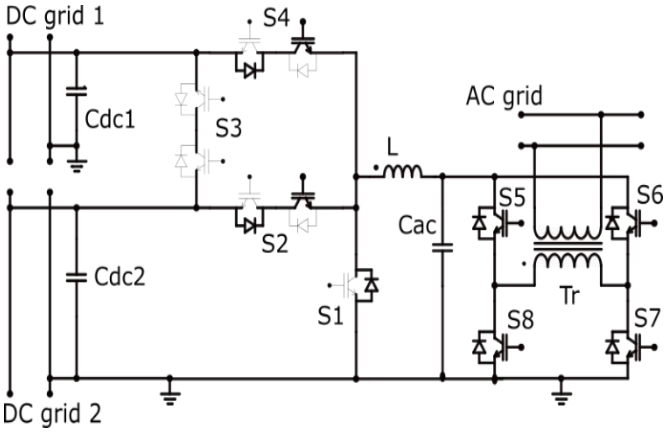

(b) Scenario 12

Fig. 13 Scenario 11 and 12 circuit principle

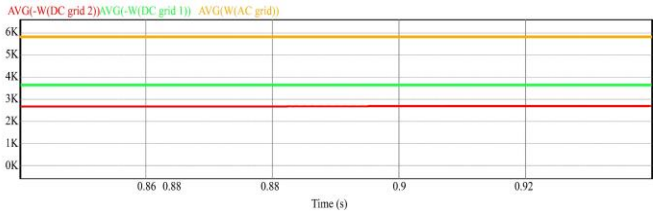

Fig. 14 Simulation graph in scenario 12

Scenario 12: the energy is supplied to the AC grid from two grids, DC1 and DC2. The converter works in two stages, with the power switch S3 inactive: The first stage works as a DC/DC converter to reduce the output voltage and current to the second stage, which operates as an H-bridge DC/AC converter. The graph in Figure 13 (b) describes the basic modes in the two stages. The simulation graph depicted in Figure 14 shows the energy value transferred from the two DC grids to the AC grid. In this case, the excess renewable energy and storage from two DC grids are connected to the AC grid.

Figure 15 describes the block diagram of the grid-connected converter control operation, with each scenario having monitoring and measuring components to make correct control decisions for each actual scenario. In the diagram, three power and voltage feedback loops are sent to the central controller to perform calculations according to the conditions from the expressions (Table 1). Table 1 shows the cases of making control decisions according to the regulations of energy conversion operation in the converter, the principle of transferring energy from one microgrid to another. The conditions (1) - (6) give the control law for the flexible converter to help optimize the energy of the sources in the grids to some extent.

Table 1. Conditions for the MGTL converter scenarios

Eq.	Expression	Corresponding scenario
1	$P_{grid-DC1}>0$; $P_{grid-DC2}<0$; $P_{grid-AC}<0$	scenarios 4, 5, 6
2	$P_{grid-DC1}>0$; $P_{grid-DC2}>0$; $P_{grid-AC}<0$	scenarios 1, 6, 12
3	$P_{grid-DC1}>0$; $P_{grid-DC2}<0$; $P_{grid-AC}>0$	scenarios 5, 9, 10
4	$P_{grid-DC1}<0$; $P_{grid-DC2}>0$; $P_{grid-AC}<0$	scenarios 1, 2, 3
5	$P_{grid-DC1}<0$; $P_{grid-DC2}>0$; $P_{grid-AC}>0$	scenarios 3, 8, 11
6	$P_{grid-DC1}<0$; $P_{grid-DC2}<0$; $P_{grid-AC}>0$	scenarios 7, 8, 9

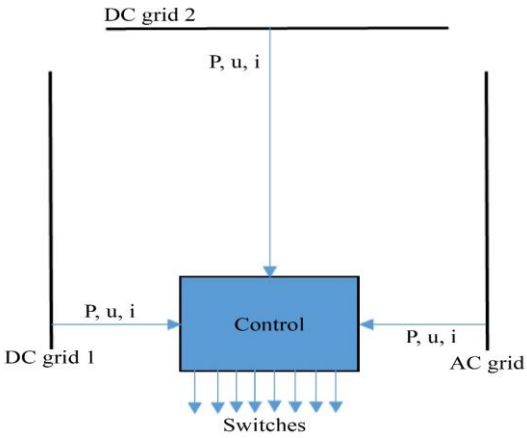

Fig. 15 Control block diagram

3. The Results of MGTL Converter

Input parameters for the simulation scenario are in Table 2 input voltages of DC and AC microgrids, corresponding loads with different values.

Table 2. Parameters of the converter simulation device

Equipment	Parameters
DC microgrid	400VDC
AC microgrid	220VAC; f=50Hz
Maximum AC load	5kW
Maximum DC load	4kW

The performance of the scenarios is shown in Figure 16 (a). The similarity is that Scenario 1 is like Scenario 6, Scenario 2 is similar to Scenario 5, Scenario 3 is similar to Scenario 4, scenario 8 is similar to Scenario 9, and Scenario 10 is similar to Scenario 11. The performance of the scenarios calculated in the simulation results is the value corresponding to the lowest value of 92% for scenarios 2 and 5, and the highest performance is 96% for scenarios 3 and 4. The capacity in the cases varies from 2-6kW. The average efficiency of energy conversion in DC/AC form is 93-95%, DC/DC conversion form has efficiency in the range of 93-96%, AC/DC conversion form has efficiency in the range of 92-94%, and the average efficiency of the converter is determined in the range of 93-95% as shown in Figure 16 (b).

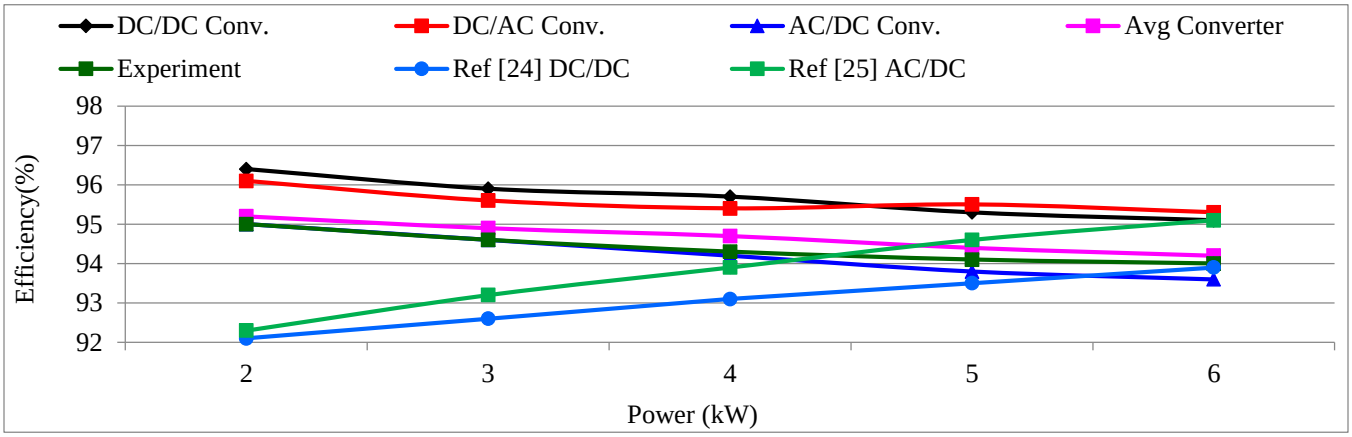

(a) Performance by transmission power value of scenarios

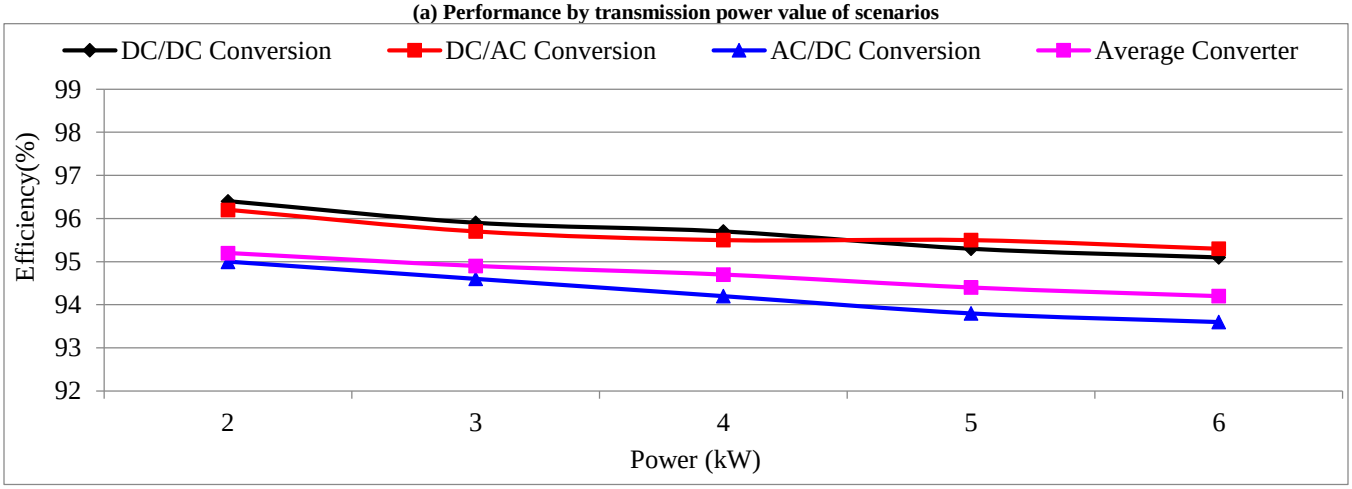

(b) Average converter efficiency

Fig. 16 Performance by transmission power

Table 3. Experimental equipment in the converter

Equipment	Parameters
Inductor L	10mH
Capacitor Ccd1, Ccd2	100uF
Capacitor Cac	47uF
Switch S1-S8	MOSFETs Q3Class HiPerFET Pwr MOSFET 500V/50A
Transformer Tr	14mH:16mH; 20A; 220VAC; f=50Hz; 6kVA
DC microgrid	400VDC
AC microgrid	220VAC; f=50Hz
Maximum AC load	5kW
Maximum DC load	4kW

3.1. Comparison of Simulation and Experimental Results

Comparing the simulation with the experimental part shows that the simulation results are almost approximate in the detailed design of the converter. The experimental part shows more clearly the values when the circuit operates in reality with different power loads. The experimental equipment is described in Table 3.

The experimental image is shown in Figure 17. Describes the components in the system and the proposed DC/AC converter connected to the DC and AC microgrids. The converter performs many functions with a simple principle to make the energy conversion process efficient. Figure 17 shows the converter, DC1, DC2 microgrids, and AC grid. The grids used are resistive loads with a maximum power of 6kW.

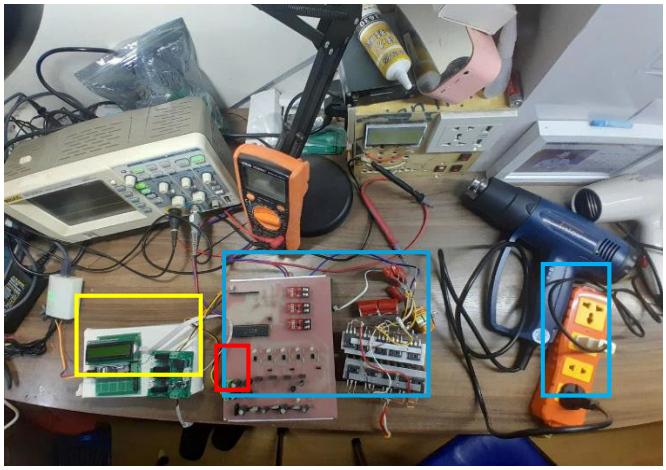

(a)

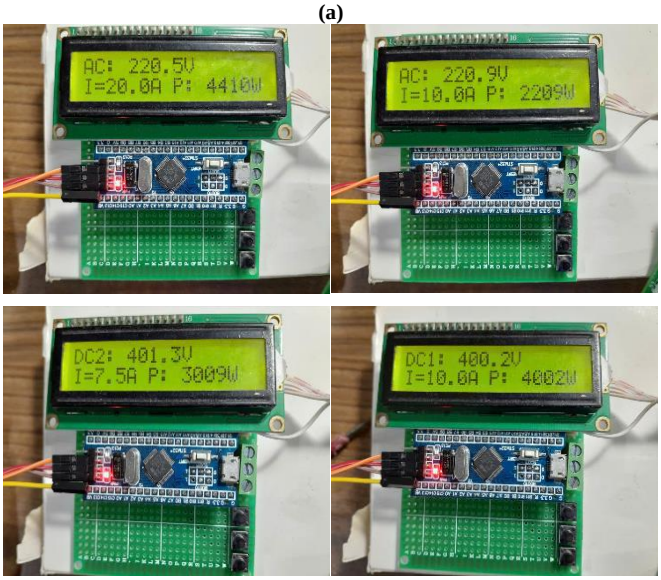

(b)

Fig. 17 Experimental images of the proposed converter: (a) experimental image of the converter, yellow frame of the measurement control block, orange frame of the converter, red frame of the DC1 and DC2 grid, blue frame of the AC grid; (b) shows the measurement of current, voltage and power values at the DC and AC grids with a capacity of 2000W-4000W

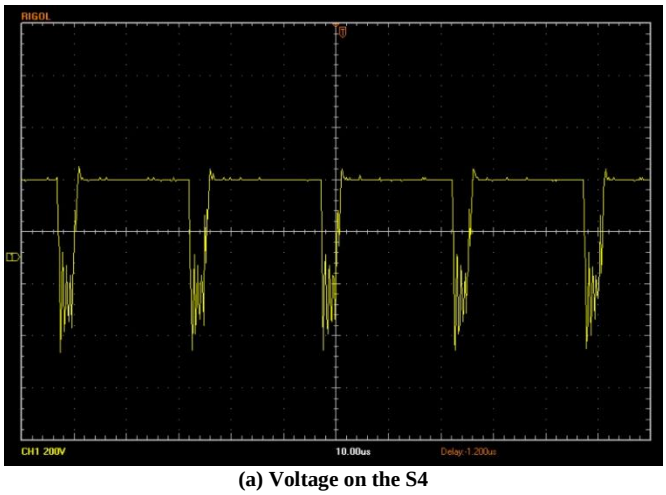

(a) Voltage on the S4

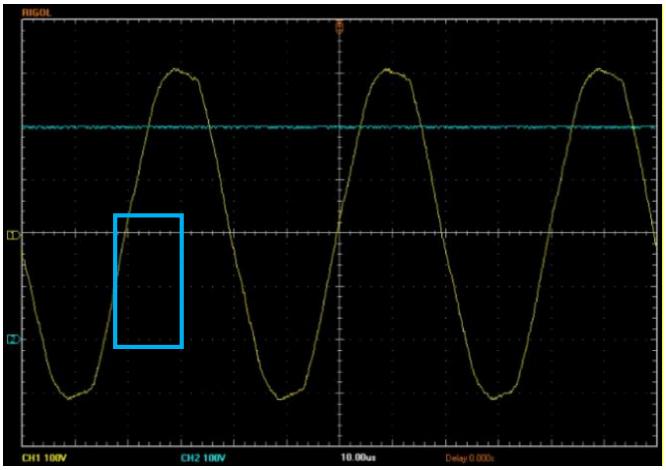

(b) DC1 voltage and AC voltage

Fig. 18 Experimental graphs of scenarios 6 and 7

Figure 18 shows the experimental results of scenarios 6 and 7 in operation and function of the converter, voltage on S4 with duty 10%, as shown in Figure 18 (a). The output voltage of the AC grid load is the yellow signal with amplitude 220V, 50Hz frequency, and the voltage on the DC1 and DC2 grids is blue with a stable voltage of nearly 400VDC, as shown in Figure 18 (b). The experimental results have been adjusted from the input selection components for the stabilized converter, and the R-L stabilized load parameters, and the elements in the power circuit converter, which are selected with good quality and good cooling for the switches in the converter. The parameter measurement process is directly and indirectly through computer-controlled measurement systems.

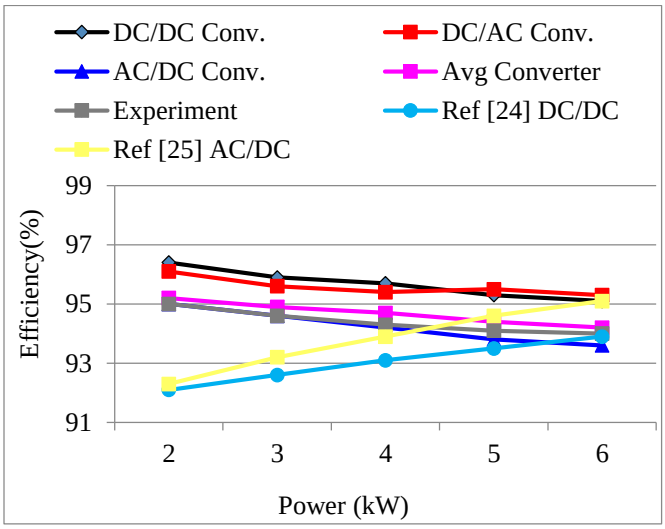

Fig. 19 Experimental and simulation comparison results

Figure 19 shows that the power conversion efficiency values from DC/DC and DC/AC have almost the same value, but the difference is more than 0.2%. The power conversion efficiency from AC/DC is much lower than that of DC/DC, with a value of 1% corresponding to each value of the conversion power. The average efficiency of the experimental

converter is larger than 95%, and the smallest is 94%; compared to the results of [19, 20] the result of the proposed converter is larger in the power range from 2-5kW. The simulation and experimental results of the proposed converter show the possibility of improving the efficiency of the multi-function converter compared to the converters with only 1-2 specific conversion functions for a load or a basic application object corresponding to a larger power than the converters in the literature [19, 20].

4. Conclusion

This paper is being carried out in the laboratory. The proposed converter presents a model for implementing the power system's connection between DC and AC microgrids. The converter structure shows that the ability to operate to convert energy from the grids is entirely flexible and feasible in two directions, capable of working independently from the grid working independently between microgrids. The resulting parameters are suitable for microgrids. This is also a good solution for optimizing distributed energy sources, stabilizing the power system, and increasing the continuity of energy supply to the load in microgrids. Moreover, there is the possibility of integrating with the smart grid using this proposed converter. The experimental and simulation results show and confirm that compared with the converter [19, 20] efficiency is improved in the load power value 2-5kW range.

Acknowledgments

The research team would like to thank the Automation and Robotics Laboratory (ARL), Posts and Telecommunications Institute of Technology, Hanoi, Vietnam, for creating favorable conditions during the implementation of the research content of this article.

References

[1] Daniel E. Olivares et al., "Trends in Microgrid Control," *IEEE Transactions on Smart Grid*, vol. 5, no. 4, pp. 1905-1919, 2014. [CrossRef] [Google Scholar] [Publisher Link]

[2] F. Martin-Martínez, A. Sánchez-Miralles, and M. Rivier, "A Literature Review of Microgrids: a Functional Layer Based Classification," *Renewable and Sustainable Energy Reviews*, vol. 62, pp. 1133-1153, 2016. [CrossRef] [Google Scholar] [Publisher Link]

[3] Dan T. Ton, and Merrill A. Smith, "The US Department of Energy's Microgrid Initiative," *The Electricity Journal*, vol. 25, no. 8, pp. 84-94, 2012. [CrossRef] [Google Scholar] [Publisher Link]

[4] Md Shafiullah et al., "Review of Recent Developments in Microgrid Energy Management Strategies," *Sustainability*, vol. 14, no. 22, pp. 1-30, 2022. [CrossRef] [Google Scholar] [Publisher Link]

[5] Altaf Q.H. Badar, and Amjad Anvari-Moghaddam, "Smart Home Energy Management System-A Review," *Advances in Building Energy Research*, vol. 16, no. 1, pp. 118-143, 2020. [CrossRef] [Google Scholar] [Publisher Link]

[6] Nikos Hatziargyriou et al., "Microgrids," *IEEE Power and Energy Magazine*, vol. 5, no. 4, pp. 78-94, 2007. [CrossRef] [Google Scholar] [Publisher Link]

[7] Yonghao Gui et al., "Passivity-Based Coordinated Control for Islanded AC Microgrid," *Applied Energy*, vol. 229, pp. 551-561, 2018. [CrossRef] [Google Scholar] [Publisher Link]

[8] Zhuangli Hu et al., "How Smart Grid Contributes to Energy Sustainability," *Energy Procedia*, vol. 61, pp. 858-861, 2014. [CrossRef] [Google Scholar] [Publisher Link]

[9] Jhojan A. Rodriguez-Gil et al., "Energy Management System in Networked Microgrids: An Overview," *Energy Systems*, pp. 1-32, 2024. [CrossRef] [Google Scholar] [Publisher Link]

[10] M. Vijayalakshmanan et al., "Microgrid Energy Management and Monitoring Systems Powered by Fuzzy Logic Maximum Power Point Tracking," *2023 5th International Conference on Inventive Research in Computing Applications (ICIRCA)*, Coimbatore, India, pp. 1727-1732, 2023. [CrossRef] [Google Scholar] [Publisher Link]

[11] Flemming Aarup, "Future Trends in DC/DC Converters for Telecommunications," *INTELEC '87 - The 9th International Telecommunications Energy Conference*, Stockholm, Sweden, pp. 55-60, 1987. [CrossRef] [Google Scholar] [Publisher Link]

[12] Andrija Stupar et al., "Multi-Objective Optimization of Multi-Level DC-DC Converters Using Geometric Programming," *IEEE Transactions on Power Electronics*, vol. 34, no. 12, pp. 11912-11939, 2020. [CrossRef] [Google Scholar] [Publisher Link]

[13] Felipe Ruiz et al., "Surveying Solid-State Transformer Structures and Controls: Providing Highly Efficient and Controllable Power Flow in Distribution Grids," *IEEE Industrial Electronics Magazine*, vol. 14, pp. 56-70, 2020. [CrossRef] [Google Scholar] [Publisher Link]

[14] Sezer Aslan, Ulas Oktay, and Nihan Altintas, "A Novel Non-Resonant Full-Bridge Multi-Output Topology for Domestic Induction Heating Applications," *Electronics*, vol. 14, no. 3, pp. 1-22, 2025. [CrossRef] [Google Scholar] [Publisher Link]

[15] Laysa L. Souza et al., "Single-Stage Isolated Half-Bridge/Full-Bridge Converter for DC/AC Applications," *2021 IEEE Energy Conversion Congress and Exposition (ECCE)*, Vancouver, BC, Canada, pp. 2359-2363, 2021. [CrossRef] [Google Scholar] [Publisher Link]

[16] Zeljko Ivanovic, and Mladen Knezic, "Modeling Push-Pull Converter for Efficiency Improvement," *Electronics*, vol. 11, no. 17, pp. 1-17, 2022. [CrossRef] [Google Scholar] [Publisher Link]

[17] Hangseok Choi, "Analysis and Design of LLC Resonant Converter with Integrated Transformer," *APEC 07 - Twenty-Second Annual IEEE Applied Power Electronics Conference and Exposition*, Anaheim, CA, USA, pp. 1630-1635, 2007. [CrossRef] [Google Scholar] [Publisher Link]

[18] Jing-Yuan Lin et al., "Analysis and Design of Three-Phase LLC Resonant Converter with Matrix Transformers," *Energies*, vol. 15, no. 4, pp. 1-18, 2022. [CrossRef] [Google Scholar] [Publisher Link]

[19] R.T. Naayagi, Andrew J. Forsyth, and R. Shuttleworth, "High-Power Bidirectional DC-DC Converter for Aerospace Applications," *IEEE Transactions on Power Electronics*, vol. 27, no. 11, pp. 4366-4379, 2012. [CrossRef] [Google Scholar] [Publisher Link]

[20] Tat-Thang LE, Ramadhan Muhammad Hakim, and Sewan Choi, "A High-Efficiency Bidirectional Single-Stage AC-DC Converter Under Wide Voltage Range for Fast Chargers," *IEEE Transactions on Power Electronics*, vol. 38, no. 4, pp. 4945-4956, 2022. [CrossRef] [Google Scholar] [Publisher Link]